Detection of Spin-Vibration States in Single Magnetic Molecules

Gregory Czap,[1] Peter J. Wagner,[1] Jie Li,[1] Feng Xue,[2] Jiang Yao,[1] R. Wu,[1,2,*] and W. Ho[1,3,†]

[1]*Department of Physics and Astronomy, University of California, Irvine, California 92697-4575, USA*
[2]*State Key Laboratory of Surface Physics and Key Laboratory of Computational Physical Sciences,*
Fudan University, Shanghai, China 200433
[3]*Department of Chemistry, University of California, Irvine, California 92697-2025, USA*

The spin states of magnetic molecules have advantageous attributes as carriers of quantum information. However, spin-vibration coupling in molecules causes a decay of excited spin states and a loss of spin coherence. Here, we detect excitations of spin-vibration states in single nickelocene molecules on Ag(110) with a scanning tunneling microscope. By transferring a nickelocene to the tip, the joint spin-vibration states with an adsorbed nickelocene were measured. Chemical variations in magnetic molecules offer the opportunity to tune spin-vibration coupling for controlling the spin coherence.

Single magnetic atoms and molecules are promising candidates for realizing the spatial limit of memory storage, spintronic devices, and qubits [1–5]. The control of the excited spin state lifetime and coherence time is essential for achieving the stability required for practical applications. Recent advances have shed light on the role of spin-vibration and spin-phonon couplings in the underbarrier relaxation of excited spin states [5–8]. These couplings have been shown both experimentally and theoretically to modulate the effective energy barrier for spin relaxation because of the static and dynamic effects [9–14]. In this context, electronic transport measurements have probed spin-vibration coupling at the single-molecule level, as electron-induced inelastic scattering events can result in excitations of spin, vibration, and spin-vibration coupled states in a molecule. Coupled spin-vibration transitions have been observed in the vibrational Kondo effect of single molecules in mechanical break junctions [15–17], single-molecule transistors [18–23], and adsorption systems [24–26]. However, an open question remains as to whether a strong resonant excitation (such as a zero bias Kondo anomaly) is required for observing spin-vibration coupled transitions.

Here, we use inelastic electron tunneling spectroscopy (IETS) with the scanning tunneling microscope (STM) [27,28] to show that the spin and vibration quanta of $S = 1$ spin triplet in nickelocene (NiCp$_2$, where Cp is cyclopentadienyl) molecules are excited simultaneously in inelastic tunneling events. Vibration peaks in IETS exhibit the Zeeman effect in the presence of an external magnetic field, indicating that they are simultaneous spin-vibration excitations. In contrast, vibration peaks of the two-nickelocene spin system are shown to correspond to transitions in which one vibration quanta and two spin quanta are simultaneously excited. Our results demonstrate that tunneling electrons can be used to excite molecules to combined spin-vibration excited states in the entirely off-resonant tunneling regime, providing a new route toward the study of the spin-vibration coupling effect in single magnetic molecules.

Experiments were performed in a homebuilt ultrahigh vacuum STM operating at a base temperature of 600 mK with an external magnetic field of up to 9 T oriented normal to the surface plane. Ag tips were prepared by electrochemical etching and repeated cycles of sputtering and annealing. The Ag(110) single crystal was prepared by sputtering with Ne$^+$ and annealing to 750 K. Nickelocene molecules were sublimed at room temperature onto the surface held at 25 K before subsequently cooling the substrate and STM to 600 mK for measurements.

Nickelocene is a spin-triplet metallocene with the degeneracy of the triplet states lifted by magnetic anisotropy, resulting in a low-spin ($m_s = 0$) ground state and high-spin ($m_s = \pm 1$) excited states [29,30]. Recent STM experiments have demonstrated that NiCp$_2$ molecules retain their $S = 1$ spin properties upon adsorption onto a metal surface or the STM tip [31–33]. NiCp$_2$ molecules adsorbed onto Ag(110) are imaged as tall elliptical donuts with the semimajor axis oriented along the [001] direction as depicted in Fig. 1(a). IETS measurements acquired with the Ag tip positioned over a single NiCp$_2$ molecule reveal strong inelastic features at 3.81 mV arising from $m_s = 0 \rightarrow m_s = \pm 1$ spin-flip excitation [Fig. 1(b)] [31–33]. The degeneracy of the $m_s = \pm 1$ spin states is lifted in an external magnetic field, resulting in the Zeeman splitting observed in IETS measurements acquired at 7 T [Fig. 1(b) bottom spectrum]. A diagram of the excited spin state energy levels is shown in Fig. 1(c). At higher bias, less intense peaks are observed and assigned to NiCp$_2$ vibration excitations. Unexpectedly, the vibration peaks are also observed to split in the magnetic field as seen in IETS measurements acquired at low field (1 T) vs high
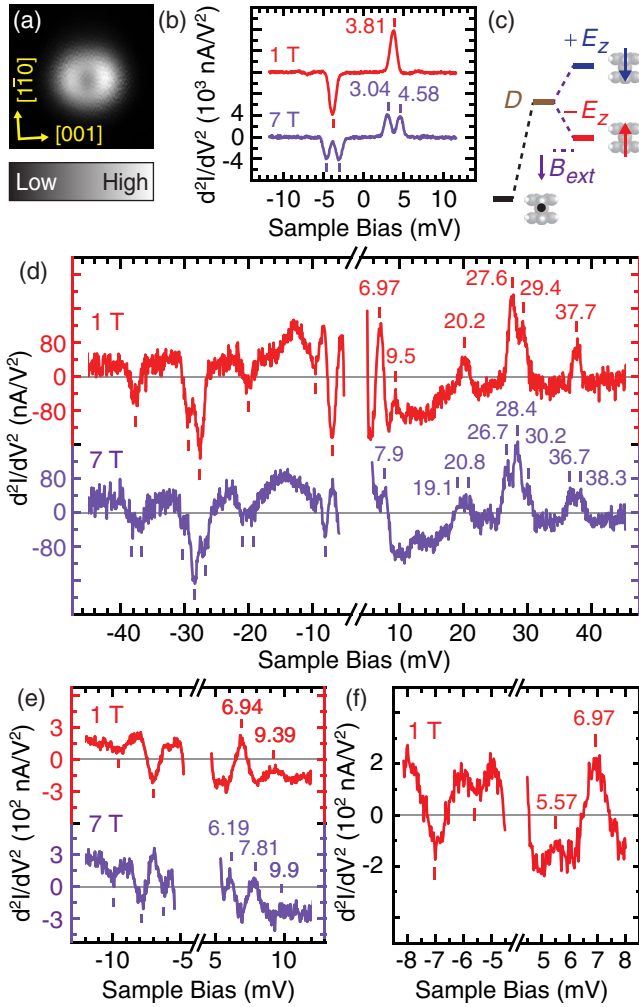
FIG. 1. Spin-vibration excitations of a single NiCp$_2$ molecule. (a) Constant-height STM topography of a single NiCp$_2$ molecule adsorbed on the Ag(110) terrace. Image size is 20×20 Å, 128×128 pixels. (b) d^2I/dV^2 measurements of the NiCp$_2$ spin-flip excitations at low (1 T) and high (7 T) magnetic field. (c) Schematic diagram depicting single NiCp$_2$ spin state energy levels with $D = 3.81$ meV and $E_Z = g\mu_B B_{ext}$. (d) d^2I/dV^2 measurements of vibration excitations at low (0 T) and high (7 T) magnetic field. Each spectrum was acquired with $800\ \mu V_{RMS}$ bias modulation at 471 Hz, average of 100 passes. To resolve the Zeeman splitting for the peaks in the 6 to 10 mV range, the IETS spectra shown in (e) were acquired with $500\ \mu V_{RMS}$ bias modulation at 471 Hz, average of 100 passes. (f) IETS spectra acquired with further reduction in bias range and $300\ \mu V_{RMS}$ bias modulation at 471 Hz to resolve the peak at 5.57 mV, average of 320 passes. All reported peak positions are the average of positive and negative bias. Gray lines in (d)–(f) indicate the zero signal position for each spectrum, which show vertical offsets originating from line shape contributions from the much more intense SSF peak.

field (7 T) [34] in Fig. 1(d). The vibration states are not expected to be affected by the magnetic field if the molecular ground state has zero net spin [39,40]. Therefore the observed Zeeman splitting indicates that the peaks

correspond to simultaneous spin-vibration excitations. These combined transitions can be described in a spin-vibration basis $|n, m_s\rangle$ as $|0, 0\rangle \rightarrow |1, \pm 1\rangle$, where n and m_s are the vibration and spin quantum numbers, respectively. Simultaneous excitations of multiple quanta are known to occur in transport measurements in the resonant tunneling regime, such as in spin-vibronic transitions of single magnetic molecules adsorbed on insulating thin films [41] where an unoccupied electronic state creates the resonant tunneling condition. More frequently they occur as inelastic spin-flip or vibration satellite peaks that accompany resonances or conductance gaps in single-molecule transport measurements, appearing near the Coulomb edge in molecular quantum dots [18,23,40,42,43], or near the superconducting energy gap if the molecule is in contact with a superconductor [44,45]. However, unlike previous studies the vibration satellites observed in the present work can be understood as inelastic satellite peaks of another inelastic transition, seemingly without the involvement of any tunneling blockade or electronic resonance state. Curiously, all the vibrational modes in the present work are observed to be spin-vibration excitations, while the vibration-only excitations are weak and seemingly absent.

To identify the vibrations observed in the IETS measurements, DFT calculations were performed with NiCp$_2$ adsorbed on the short bridge site of the Ag(110) slab in agreement with the optimized binding site established in previous work [33] (see Supplemental Material for details of the DFT calculations [34]). The calculated vibration modes and energies in the 0–50 meV range are shown in Fig. 2. Good agreement with experiment is found only if the magnetic anisotropy energy ($D = 3.81$ meV) is added to the calculated vibration energy $\hbar\omega$, as shown in Fig. 2(i). Since the vibration peaks observed in Fig. 1(d) are transitions to simultaneous spin-vibration excited states, and the spin-only transitions require an energy D, the spin-vibration states evidently require $D + \hbar\omega$ to excite with tunneling electrons.

A schematic diagram depicting the energy levels and types of excitations for a NiCp$_2$ molecule on Ag(110) is shown in Figs. 3(a)–3(d). In the experimental geometry indicated in Fig. 3(a), the NiCp$_2$ molecule adsorbs upright on the surface, and both the external magnetic field and spin hard axis align along the surface normal. Without the spin-vibration coupling, the molecules may undergo either spin-flip excitations as in Fig. 3(b) or vibration excitations as in Fig. 3(c). The energy levels are then depicted in Fig. 3(d), with high-spin excited states elevated by the magnetic anisotropy energy D relative to the ground state and excited vibration states elevated by $\hbar\omega$. In addition, combined spin-vibration excited states exist at energy $D + \hbar\omega$, exactly as we observed in Fig. 2(i). In an external magnetic field, the vibration-only energy levels are unaffected while the Zeeman effect lifts the degeneracy of the high-spin and spin-vibration states, resulting in Zeeman splitting $\pm E_Z = \pm g\mu_B B_{ext}$, as shown in Fig. 3(d).
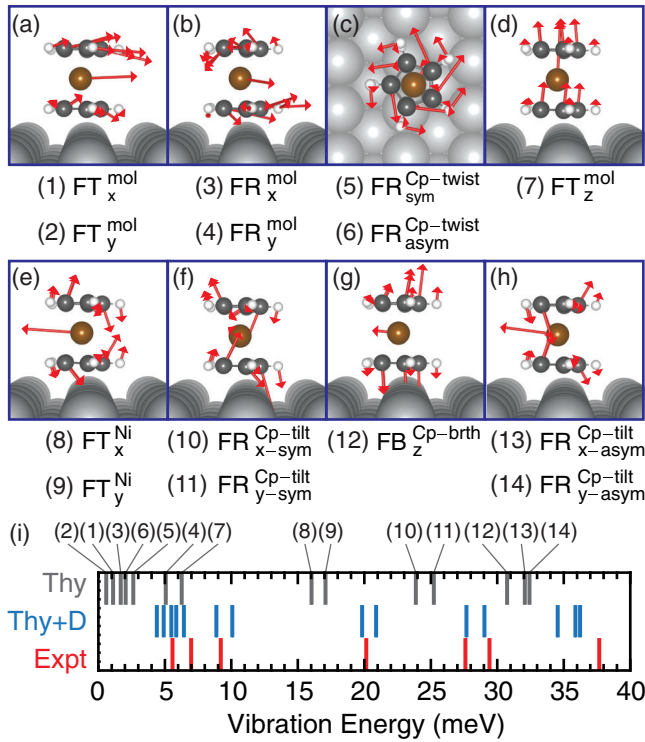
FIG. 2. Comparison of vibration energies calculated by DFT with experimental data. (a)–(h) Calculated vibration modes in the 0–50 meV range. (i) Comparison of measured peak positions (red) with calculated excitation energies that either includes (blue) or excludes (gray) an energy offset equal to the magnetic anisotropy energy D.

Now we extend our discussion to a two-NiCp$_2$ system, which can be created by functionalizing the STM tip with a NiCp$_2$ molecule and positioning it over another surface-adsorbed NiCp$_2$ molecule as depicted in Fig. 3(e). Recent experiments have shown that a two-NiCp$_2$ spin system can undergo both single spin-flip (SSF) and double spin-flip (DSF) excitations [31–33], with simplified depictions of states and energy diagrams shown in Figs. 3(f) and 3(g). Note that only the antiferromagnetic ($\Delta m_{\mathrm{TOT}} = 0$) DSF excitation is possible due to spin angular momentum selection rules imposed by the spin $\frac{1}{2}$ tunneling electron which forbid ferromagnetic ($\Delta m_{\mathrm{TOT}} = \pm 2$) DSF excitations. A previous study demonstrated that the spins of the two molecules couple via antiferromagnetic exchange interactions, resulting in zero-field splitting of the SSF peaks and redshifting of the DSF peaks [33]. The degeneracy of the SSF states can be lifted at zero field by $2J$ from the exchange interaction and can split further by $2E_Z$ from the Zeeman effect if an external magnetic field is applied. The antiferromagnetic DSF states, on the other hand, can be slightly redshifted by $-\delta$ due to exchange interactions but remain unchanged in an external magnetic field because of the net zero magnetic moment [33]. We want to emphasize that the energy levels depicted in Fig. 3(g) are simplified for clarity, as the eigenfunctions of the spin Hamiltonian are
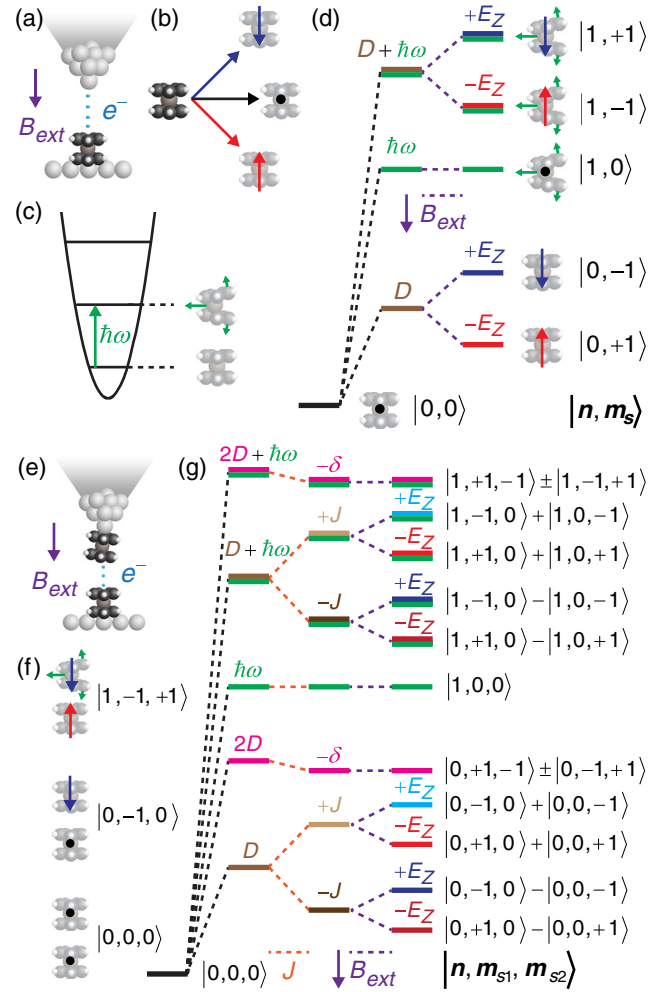

FIG. 3. Schematic diagrams of the spin, vibration, and spin-vibration energy levels of the one and two NiCp$_2$ spin systems. (a) Experimental geometry for single NiCp$_2$. (b) Depiction of spin-flip excitation and (c) vibration excitation. (d) Simplified energy level diagram for NiCp$_2$ excited states in the $|n, m_s\rangle$ basis. (e) Experimental geometry for two NiCp$_2$. (f) Example of the $|n, m_{s1}, m_{s2}\rangle$ basis for two molecules. Here, the vibration quantum number n refers to a vibration mode of one of the two molecules, such as the NiCp$_2$ adsorbed on the tip. (g) Simplified energy level diagram for the two-NiCp$_2$ excited states.

usually mixtures of bases $|m_{s1}, m_{s2}\rangle$. A complete description is included in the Supplemental Material of both [33] (Fig. S4 and Table S1) and the present work [34]. The vibrationally excited levels consist of vibration-only, SSF + vibration and DSF + vibration states. In the absence of external magnetic field or exchange interactions, the SSF + vibration states are D higher in energy than the vibration-only states, and the DSF + vibration states are blueshifted by $2D$. The spin + vibration states are all affected by exchange interactions, causing the same zero-field splitting of the SSF + vibration states and redshift of the DSF + vibration states as seen in the spin-only excited states. Importantly, the SSF + vibration states respond to an external magnetic field while the DSF + vibration states

do not, which combined with the energy offsets of D and $2D$, respectively, relative to the vibration-only states permits their unambiguous identification. Here, we assume for simplicity that vibrations in the two molecules are decoupled and have the same energies.

To determine which vibrational states can be experimentally accessed in the two-NiCp$_2$ system, a NiCp$_2$ tip was prepared by positioning the Ag tip over a NiCp$_2$ molecule and controllably advancing the tip toward the surface, resulting in a transfer of the molecule to the tip. The resulting NiCp$_2$ tip was then positioned over another NiCp$_2$ molecule on the surface [depicted in Fig. 4(a) inset] and spectroscopic measurements were performed [Figs. 4(a) and 4(b)]. The spectra reveal three low energy excitations, with the first two corresponding to SSF excitations and the third, more intense peak corresponding to the antiferromagnetic DSF excitation [33]. The ~1.8 mV splitting of the SSF peak at low magnetic field indicates an exchange energy of ~0.9 meV at this tip-surface separation [33]. As in the single NiCp$_2$ case, vibration excitations appear as much weaker peaks at higher energies as shown in Fig. 4(c). However, in contrast to the single NiCp$_2$ case, the vibration peaks of the two-NiCp$_2$ system *do not* split in an applied magnetic field. High resolution IETS measurements of the ~35 meV vibration for the single NiCp$_2$ molecule acquired with the Ag tip at $B = 0$ T and $B = 9$ T are shown in Fig. 4(d) while similar measurements for the two-NiCp$_2$ system are shown in Fig. 4(e). While the single-molecule vibrations have a pronounced splitting at high field, the two-molecule vibrations are seemingly unaffected. In addition, all the vibrations of the two-molecule system appear blueshifted by ~3.5 meV with respect to the values measured for the single NiCp$_2$ case, in good agreement with the expected blueshift of ~3.6 meV which arises from the magnetic anisotropy energy of the tip NiCp$_2$ ($D_{tip} = 4$ meV) with an exchange-induced redshift ($-\delta = 0.4$ meV) (see Supplemental Material for an expanded discussion [34]). The vibration excitations of the two-molecule system correspond to DSF + vibration states in which both molecules' spins have been flipped in opposite directions and a vibration has been excited *simultaneously*. Although the spin and vibration degrees of freedom are combined in a rigorous sense, one may still view this observation as evidence of inelastic excitations of three different quanta by one tunneling electron. The transition for this peak can be represented in the two-molecule spin-vibration basis $|n, m_{s1}, m_{s2}\rangle$ as $|0, 0, 0\rangle \rightarrow (1/\sqrt{2})(|1, \pm1, \mp1\rangle \pm |1, \mp1, \pm1\rangle)$, where n, m_{s1}, and m_{s2} are the vibration, tip-spin, and surface-spin quantum numbers, respectively, and depicted as the highest energy level in Fig. 3(g).

The remarkable fact that only DSF + vibration states are observed in the two-molecule system implies that the inelastic cross sections for the other possible vibration states [SSF + vibration or vibration only in Fig. 3(g)] are somehow much lower in comparison. The overall conductance
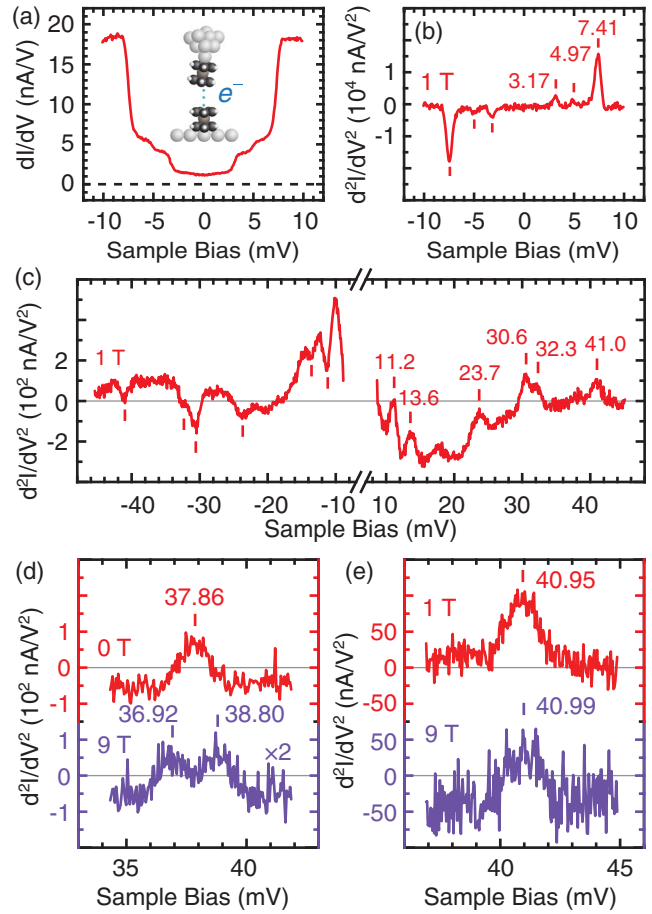

FIG. 4. Spin-vibration excitations of the two-NiCp$_2$ spin system. (a) dI/dV and (b) d^2I/dV^2 measurements of NiCp$_2$ tip/NiCp$_2$ surf. The two lower energy peaks correspond to SSF excitations, with zero-field degeneracy lifted by intermolecular exchange interactions. The 7.41 mV peak corresponds to an antiferromagnetic DSF excitation. (c) Vibrational spectrum of NiCp$_2$ tip/NiCp$_2$ surf. The observed vibration modes are similar to those found in the single NiCp$_2$ measurements [Fig. 1(d)] except that they are all blueshifted by 3 to 4 mV. Spectra were acquired with 800 μV$_{RMS}$ bias modulation and an average of 50 passes. (d) Enlargement of the ~38 mV vibration of the single NiCp$_2$ molecule acquired with Ag tip at low magnetic field (0 T, red) and high magnetic field (9 T, purple) showing Zeeman splitting. (e) Similar measurements of the same vibration for the two-NiCp$_2$ system at low field (1 T, red) and high field (9 T, purple) showing ~3 meV blueshift and the absence of Zeeman splitting. The spectra shown in (d) and (e) were acquired with 800 μV$_{RMS}$ bias modulation and an average of 80 passes.

change for the DSF excitation is around three to four times that of each SSF excitation and is around ten times higher than the no spin-flip conductance channel [Fig. 4(a)]. The tunneling electrons are participating in DSF over the other excitations at elevated bias. The DSF + vibration excitations then become the most favored tunneling channels for vibration excitations so that only these can be resolved in the experiment. This interpretation can also account for the observation of only SSF + vibration states in the single

NiCp$_2$ case, since the conductance of the SSF tunneling channel is similarly much higher than the no spin-flip channel [34]. The results presented here also raise questions about the degree to which spin-vibration [9,11,13] and electron-vibration [17,21,46] couplings are important in determining the intensity of inelastic satellite peaks in the off-resonant tunneling regime. Notably, recent STM-IETS measurements of a Ni-NiCp$_2$ complex embedded in a NiCp$_2$ monolayer on Cu(100) revealed strong peaks at elevated bias which were assigned to vibrationally assisted spin excitations similar to those discussed in the present work [47]. The much larger intensity of spin-vibration peaks found in the Ni-NiCp$_2$ complex than for the single NiCp$_2$ and two-NiCp$_2$ systems indicate a clear need for novel theoretical treatments.

In summary, we have demonstrated that tunneling electrons of the STM can be used to excite combined spin-vibration transitions in single magnetic molecules. The presence (or absence) of Zeeman splitting in an external magnetic field along with DFT calculations of the vibration energies reveal that the observed inelastic tunneling spectra of single NiCp$_2$ molecules correspond to simultaneous excitations of one spin quanta and one vibration quanta. Furthermore, the observed vibration peaks of the two-NiCp$_2$ spin system are simultaneous excitations of two spin quanta and one vibration quanta. These results show a more complex magnetic field response than observed previously because of the presence of double spin-flip and spin-vibration combined states. As spin-vibration combined states are expected in almost all magnetic molecules and are predicted to be sensitive to spin-vibration coupling [9,11,13], our findings may provide a route to characterizing the spin relaxation pathways which strongly influence quantum coherence of qubits based on magnetic molecules.

*Corresponding author.
wur@uci.edu
†Corresponding author.
wilsonho@uci.edu

[1] L. Bogani and W. Wernsdorfer, Nat. Mater. **7**, 179 (2008).
[2] Y.-S. Ding, Y.-F. Deng, and Y.-Z. Zheng, Magnetochemistry **2**, 40 (2016).
[3] F. Donati, S. Rusponi, S. Stepanow, C. Wäckerlin, A. Singha, L. Persichetti, R. Baltic, K. Diller, F. Patthey, E. Fernandes, J. Dreiser, Ž. Šljivančanin, K. Kummer, C. Nistor, P. Gambardella, and H. Brune, Science **352**, 318 (2016).
[4] E. Moreno-Pineda, C. Godfrin, F. Balestro, W. Wernsdorfer, and M. Ruben, Chem. Soc. Rev. **47**, 501 (2018).
[5] L. Escalera-Moreno, J. J. Baldoví, A. Gaita-Ariño, and E. Coronado, Chem. Sci. **9**, 3265 (2018).
[6] M. Ganzhorn, S. Klyatskaya, M. Ruben, and W. Wernsdorfer, Nat. Nanotechnol. **8**, 165 (2013).
[7] A. Lunghi, F. Totti, R. Sessoli, and S. Sanvito, Nat. Commun. **8**, 14620 (2017).
[8] C. A. P. Goodwin, F. Ortu, D. Reta, N. F. Chilton, and D. P. Mills, Nature **548**, 439 (2017).
[9] S. Kokado, K. Harigaya, and A. Sakuma, J. Phys. Soc. Jpn. **79**, 114721 (2010).
[10] J. J. Parks, A. R. Champagne, T. A. Costi, W. W. Shum, A. N. Pasupathy, E. Neuscamman, S. Flores-Torres, P. S. Cornaglia, A. A. Aligia, C. A. Balseiro, G. K.-L. Chan, H. D. Abruña, and D. C. Ralph, Science **328**, 1370 (2010).
[11] F. May, M. R. Wegewijs, and W. Hofstetter, Beilstein J. Nanotechnol. **2**, 693 (2011).
[12] D. A. Ruiz–Tijerina, P. S. Cornaglia, C. A. Balseiro, and S. E. Ulloa, Phys. Rev. B **86**, 035437 (2012).
[13] A. Kenawy, J. Splettstoesser, and M. Misiorny, AIP Adv. **7**, 055708 (2017).
[14] L. Escalera-Moreno, N. Suaud, A. Gaita-Ariño, and E. Coronado, J. Phys. Chem. Lett. **8**, 1695 (2017).
[15] J. J. Parks, A. R. Champagne, G. R. Hutchison, S. Flores-Torres, H. D. Abruña, and D. C. Ralph, Phys. Rev. Lett. **99**, 026601 (2007).
[16] D. Rakhmilevitch, R. Korytár, A. Bagrets, F. Evers, and O. Tal, Phys. Rev. Lett. **113**, 236603 (2014).
[17] P. Roura-Bas, L. Tosi, and A. A. Aligia, Phys. Rev. B **93**, 115139 (2016).
[18] J. Park, A. N. Pasupathy, J. I. Goldsmith, C. Chang, Y. Yaish, J. R. Petta, M. Rinkoski, J. P. Sethna, H. D. Abruña, P. L. McEuen, and D. C. Ralph, Nature **417**, 722 (2002).
[19] W. Liang, M. P. Shores, M. Bockrath, J. R. Long, and H. Park, Nature **417**, 725 (2002).
[20] L. H. Yu, Z. K. Keane, J. W. Ciszek, L. Cheng, M. P. Stewart, J. M. Tour, and D. Natelson, Phys. Rev. Lett. **93**, 266802 (2004).
[21] J. Paaske and K. Flensberg, Phys. Rev. Lett. **94**, 176801 (2005).
[22] P. S. Cornaglia, G. Usaj, and C. A. Balseiro, Phys. Rev. B **76**, 241403(R) (2007).
[23] F. Reckermann, M. Leijnse, and M. R. Wegewijs, Phys. Rev. B **79**, 075313 (2009).
[24] I. Fernández-Torrente, K. J. Franke, and J. I. Pascual, Phys. Rev. Lett. **101**, 217203 (2008).
[25] T. Choi, S. Bedwani, A. Rochefort, C.-Y. Chen, A. J. Epstein, and J. A. Gupta, Nano Lett. **10**, 4175 (2010).
[26] A. Mugarza, C. Krull, R. Robles, S. Stepanow, G. Ceballos, and P. Gambardella, Nat. Commun. **2**, 490 (2011).
[27] B. C. Stipe, M. A. Rezaei, and W. Ho, Science **280**, 1732 (1998).
[28] A. J. Heinrich, J. A. Gupta, C. P. Lutz, and D. M. Eigler, Science **306**, 466 (2004).
[29] R. Prins, J. D. W. van Voorst, and C. J. Schinkel, Chem. Phys. Lett. **1**, 54 (1967).
[30] P. Baltzer, A. Furrer, J. Hulliger, and A. Stebler, Inorg. Chem. **27**, 1543 (1988).
[31] M. Ormaza, N. Bachellier, M. N. Faraggi, B. Verlhac, P. Abufager, P. Ohresser, L. Joly, M. Romeo, F. Scheurer, M.-L. Bocquet, N. Lorente, and L. Limot, Nano Lett. **17**, 1877 (2017).

[32] M. Ormaza, P. Abufager, B. Verlhac, N. Bachellier, M.-L. Bocquet, N. Lorente, and L. Limot, Nat. Commun. **8,** 1974 (2017).

[33] G. Czap, P. J. Wagner, F. Xue, L. Gu, J. Li, J. Yao, R. Wu, and W. Ho, Science **364,** 670 (2019).

[34] See Supplemental Material at http://link.aps.org/supplemental/10.1103/PhysRevLett.123.106803 for details of DFT calculations, additional data, discussions, and table, which includes Refs. [33,35–38].

[35] J. P. Perdew, K. Burke, and M. Ernzerhof, Phys. Rev. Lett. **77,** 3865 (1996).

[36] P. E. Blöchl, Phys. Rev. B **50,** 17953 (1994).

[37] G. Kresse and D. Joubert, Phys. Rev. B **59,** 1758 (1999).

[38] Z. Han, G. Czap, C. Xu, C. L. Chiang, D. Yuan, R. Wu, and W. Ho, Phys. Rev. Lett. **118,** 036801 (2017).

[39] H. B. Heersche, Z. de Groot, J. A. Folk, H. S. J. van der Zant, C. Romeike, M. R. Wegewijs, L. Zobbi, D. Barreca, E. Tondello, and A. Cornia, Phys. Rev. Lett. **96,** 206801 (2006).

[40] E. Burzurí, R. Gaudenzi, and H. S. J. van der Zant, J. Phys. Condens. Matter **27,** 113202 (2015).

[41] U. Ham and W. Ho, Phys. Rev. Lett. **108,** 106803 (2012).

[42] H. Park, J. Park, A. K. L. Lim, E. H. Anderson, A. P. Alivisatos, and P. L. McEuen, Nature **407,** 57 (2000).

[43] M.-H. Jo, J. E. Grose, K. Baheti, M. M. Deshmukh, J. J. Sokol, E. M. Rumberger, D. N. Hendrickson, J. R. Long, H. Park, and D. C. Ralph, Nano Lett. **6,** 2014 (2006).

[44] B. W. Heinrich, L. Braun, J. I. Pascual, and K. J. Franke, Nat. Phys. **9,** 765 (2013).

[45] B. W. Heinrich, L. Braun, J. I. Pascual, and K. J. Franke, Nano Lett. **15,** 4024 (2015).

[46] M. C. Lüffe, J. Koch, and F. von Oppen, Phys. Rev. B **77,** 125306 (2008).

[47] N. Bachellier, B. Verlhac, L. Garnier, J. Zaldívar, C. Rubio-Verdú, P. Abufager, M. Ormaza, D.-J. Choi, M.-L. Bocquet, J. I. Pascual, N. Lorente, and L. Limot, arXiv:1906.00660.